Int J CARS (2013) 8:75–86
DOI 10.1007/s11548-012-0691-8

ORIGINAL ARTICLE

Surgical bedside master console for neurosurgical robotic system

Jumpei Arata · Hajime Kenmotsu · Motoki Takagi · Tatsuya Hori · Takahiro Miyagi · Hideo Fujimoto · Yasukazu Kajita · Yuichiro Hayashi · Kiyoyuki Chinzei · Makoto Hashizume

Received: 10 January 2012 / Accepted: 10 April 2012 / Published online: 15 May 2012

Abstract
Purpose We are currently developing a neurosurgical robotic system that facilitates access to residual tumors and improves brain tumor removal surgical outcomes. The system combines conventional and robotic surgery allowing for a quick conversion between the procedures. This concept requires a new master console that can be positioned at the surgical bedside and be sterilized.
Methods The master console was developed using new technologies, such as a parallel mechanism and pneumatic sensors. The parallel mechanism is a purely passive 5-DOF (degrees of freedom) joystick based on the author's haptic research. The parallel mechanism enables motion input of conventional brain tumor removal surgery with a compact, intuitive interface that can be used in a conventional surgical environment. In addition, the pneumatic sensors implemented on the mechanism provide an intuitive interface and electrically isolate the tool parts from the mechanism so they can be easily sterilized.
Results The 5-DOF parallel mechanism is compact (17 cm width, 19 cm depth, and 15 cm height), provides a 505,050 mm and 90° workspace and is highly backdrivable (0.27 N of resistance force representing the surgical motion). The evaluation tests revealed that the pneumatic sensors can properly measure the suction strength, grasping force, and hand contact. In addition, an installability test showed that the master console can be used in a conventional surgical environment.
Conclusion The proposed master console design was shown to be feasible for operative neurosurgery based on comprehensive testing. This master console is currently being tested for master-slave control with a surgical robotic system.

Keywords Neurosurgery · Surgical robot · Master console · Brain tumor resection

J. Arata · M. Takagi · T. Hori · T. Miyagi · H. Fujimoto
Nagoya Institute of Technology, Gokiso-cho, Showa-ku, Nagoya 466-8555, Japan
e-mail: jumpei.arata@me.com

H. Kenmotsu (✉) · M. Hashizume
Kyushu University, Maidashi 3-1-1, Higashi-ku, Fukuoka 812-8582, Japan
e-mail: kenken@dem.med.kyushu-u.ac.jp

Y. Kajita · Y. Hayashi
Department of Neurosurgery, Graduate School of Medicine, Nagoya University, 65 Tsurumai-cho, Showa-ku, Nagoya 466-8550, Japan

K. Chinzei
National Institute of Advanced Industrial Science and Technology, 1-2-1 Namiki, Tsukuba 305-8564, Japan

Purpose

Background

In brain tumor removal surgery, the tumor removal rate is related to the clinical outcome. According to "Report of Brain Tumor Registry of Japan [1]," the 5-year survival rate for malignant glioma (in 6,398 patients) was 40 % for complete removal, 22 % for 95 % or more removal, and 10–15 % for under 95 % removal. Surgery is the most important procedure, representing the first step in the treatment of glioma, and is performed with the aim of complete removal of the lesion while preserving neurological function. Cutting-edge technologies such as image-guided surgery and intraoperative fluorescence diagnostics using 5-aminolevulinic acid (5-ALA) improve the tumor removal rate, although high levels of surgical skill are still required in cases where the tumor is located in the proximity of neural structures. However, even

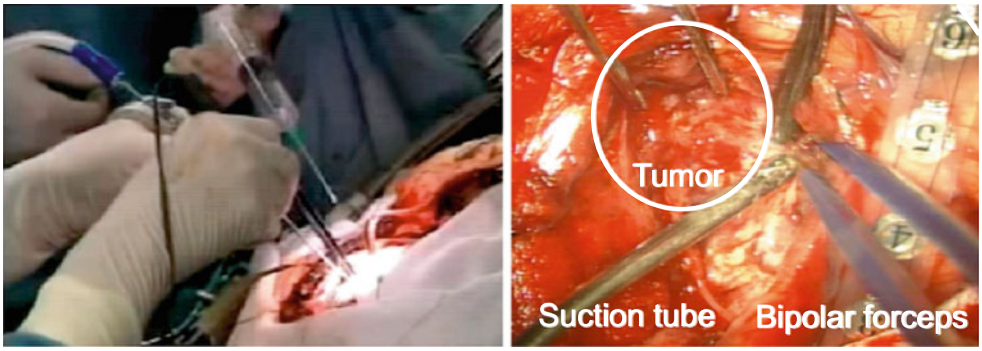

Fig. 1 These pictures show the surgical brain tumor removal procedure in conventional surgery. In such procedures, a suction tube and bipolar forceps are commonly used. The *left picture* shows the close proximity of the surgeon's hands to the patient during the surgery. The *right picture* shows the surgical field through a microscope

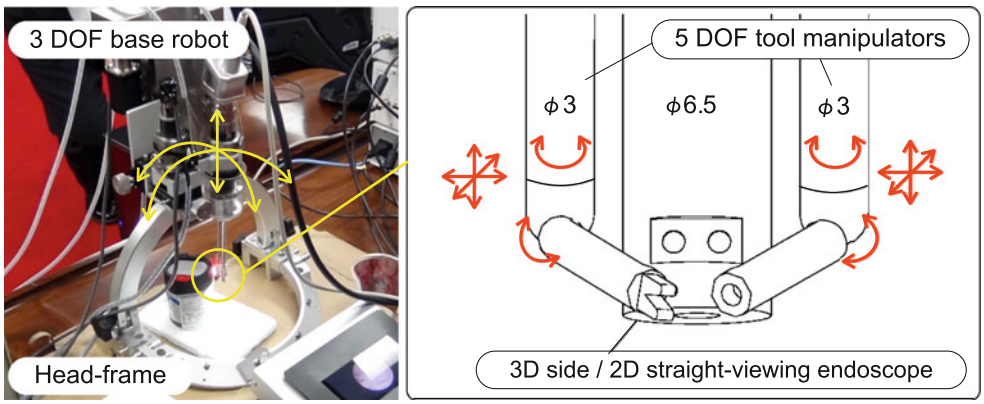

Fig. 2 The *left picture* shows an overview of the robotic system under development for brain tumor removal. The *right picture* shows the tool manipulators and endoscope implemented on the tip of the robot

with these new techniques, there are still many cases where the lesion is not accessible by the surgeon. In our research group, a surgical robotic system for brain tumor removal is currently in development for complete brain tumor removal. The system is being developed to provide improved accessibility to lesions that are located deep inside or on the interior wall of a brain cavity. In this study, we introduce a newly developed master console for the robotic system.

The robotic system for tumor removal is currently in development and can remove tumors that remain after conventional brain tumor removal surgery due to limited accessibility. In conventional brain tumor removal surgery, the surgeon typically removes the tumor using a suction tube and bipolar forceps by means of the microscope image (Fig. 1). The removed tumor area then commonly forms a cavity. In the case where the cavity is located in the proximity of neural structures, the removal procedure becomes difficult with respect to brain function preservation. Thus, the surgeon must perform tumor removal while avoiding damage to the surrounding healthy tissue. The operation becomes even more difficult due to the limited accessibility of surgical tools to the lesion. In the case where the tumor still remains in the brain cavity (e.g., the tumor is located behind the neural structure or is stuck on the internal wall of a cavity), the tumor cannot be seen with the microscope and is not accessible using conventional surgical tools. Based on this background information, we are developing a robotic system that improves the accessibility to residual tumors.

The robotic system consists of a base robot, a 3D side/2D straight-viewing endoscope and a dual-tool manipulator (Fig. 2). The base robot has three degrees of freedom (DOF) and can be attached to a conventional head frame. The endoscope and two tool manipulators are attached to the base robot and can be put into a brain cavity through a gyrus in a minimally invasive manner. The endoscope allows us to have a 3D side view and a 2D straight view, and the viewing mode can be switched manually during the procedure (e.g., the 2D straight view is used for inserting the device into the cavity, and the 3D side view is used for the tumor removal procedure). In addition, the 3D side view is compatible with 5-ALA to detect the tumor location. The tool manipulators have 5-DOF for each manipulator and can be equipped with

bipolar forceps and a suction tube. The tips of the manipulators are bendable to over 90°, and therefore, the robot can perform the tumor removal in a brain cavity. The most advantageous features of the robot are its compact size and its ability to be easily mounted on a conventional surgical head frame, which enable quick conversions between conventional and robotic surgery. Therefore, the concept of the robotic system is a combination of conventional and robotic surgery that can provide improved accessibility to the lesions.

The robotic system concept described earlier requires the development of a new master console. To be used in conventional brain tumor removal surgery, the master console must be compatible with a conventional surgical setup. In addition, to achieve quick and smooth conversions between conventional and robotic surgery, the master console must be sterilizable and manipulable using surgical gloves. An intuitive interface based on conventional surgical procedures is also required. In this study, we propose a new master console based on the requirements above, introducing a new parallel mechanism and pneumatic sensors.

Related research

In recent years, robotic technology has been introduced into many neurosurgical procedures [2,3].

First, robotic technology was introduced into neurosurgery in image-guided devices. One such example is Neuromate [4] (Renishow, UK), which is a commercial neurosurgical robot that enables precise positioning of a cannula or probe for biopsies or for targeting deep brain structures using computed tomography (CT) and magnetic resonance imaging (MRI) images. Pathfinder [5] (Prosurgics, UK) is another example of an image-guided surgical robot. In these image-guided robots, robotic technology has been introduced for precise positioning. Therefore, the robots are essentially controlled using the coordinates generated by the controller based on medical images.

Then, robotic technology was introduced to improve the limited accessibility to the lesion and to extend the surgeon's dexterity. Da Vinci [6] (Intuitive Surgical, US) is a well-known example that incorporates these features. In this case, the surgical robot is controlled based on a master-slave system; thus, the robot performs the surgery based on the coordinates given by the surgeon's motion input through the master console. In the neurosurgical field, Sutherland et al. presented NeuroArm, which is equipped with two MRI-compatible robotic arms [7]. In NeuroArm, the console is equipped based on a conventional haptic device known as Phantom (Sensable Technology, US [8]). Morita et al. presented a micro-neurosurgery robotic arm for treating deep brain areas [9]. The system was developed to perform micro-manipulations (e.g., ligation of microscopic blood vessels) in a deep surgical field. The master console was implemented for a dual 7-DOF manipulator-type robot taking into account the micro-manipulations. Goto et al. [10] presented NeuRobot, which is a master-slave micro-manipulator system for neurosurgery. The robot consists of a 3D endoscope and three robotic arms. For NeuRobot, the master console was implemented using a pair of conventional revolute levers and switches. Authors also presented a neurosurgical robotic system using master-slave technology in their past study [11].

In addition, the master console mechanism has been widely explored in haptic research. The author also studied haptic devices and reported a survey of previously presented devices in [12].

The main challenge of the presented study of master consoles is the compatibility with conventional brain tumor removal surgery. None of the previous studies have focused on the integration of conventional and robotic surgery; therefore, the patient and master console have been placed a certain distance apart in these systems. In this study, we propose a new master console by combining conventional and robotic procedures.

Material and methods

The developed master console consists of a 3D viewer to provide the surgical view, a navigation monitor, two master manipulators, a control unit, and foot switches (illustrated in the left panel of Fig. 3). All of these components were implemented in a desktop style to be fitted at the surgical bedside in an operating room. The size of the device is 300 mm in width, 300 mm in depth, and 830 mm in height. The positions of the 3D viewer, navigation monitor, and master manipulators are adjustable for different operators and surgical environments.

The master manipulators were designed to realize an intuitive motion input based on conventional brain tumor removal surgery, as illustrated in Fig. 1. The master manipulator consists of a parallel mechanism and a tool part. As shown in the right panels of Fig. 3, the operator handles the tool parts of the master manipulators by putting his or her palms on the palm rest. It should be noted that the surgeon's hands are commonly positioned close together in conventional surgery. Therefore, the manipulators were designed to position the right and left hands close together by introducing a newly developed parallel mechanism that avoids the problematic mechanical interference that commonly occurs in conventional mechanisms. The parallel mechanism is equipped with optical encoders and electromagnetic brakes. The brakes are used for locking the position and rotation of the master manipulator. The tool part is equipped with bipolar forceps and a suction tube for each hand and can be handled like conventional neurosurgical tools. The tool part can be fixed to each manipulator over a surgical nylon drape using a pair of Neodymium magnets. In addition, new pneumatic

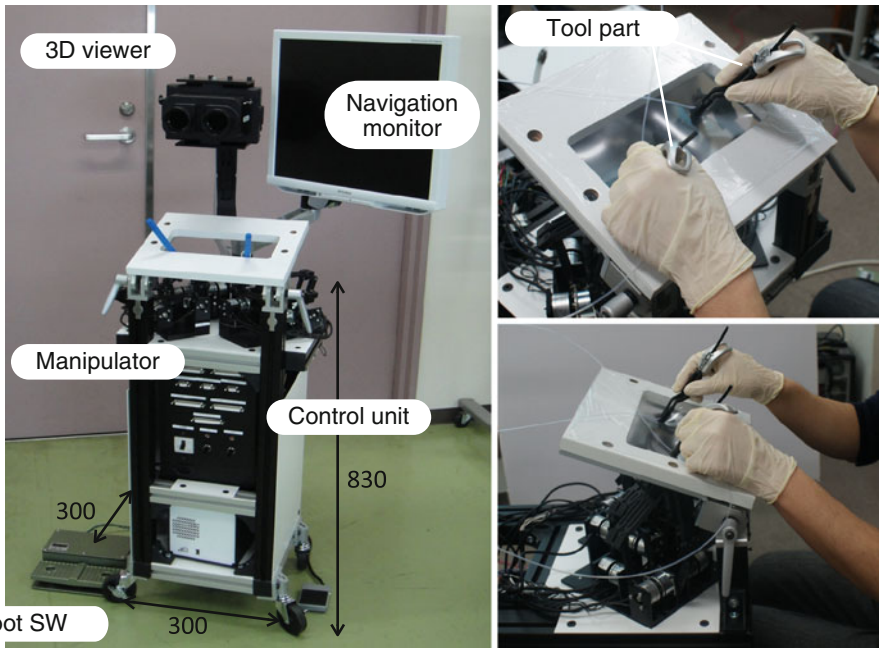

Fig. 3 The pictures show an overview of the developed master console. The *left picture* shows the device setup, and the *right pictures* show an operator handling the master manipulators

sensors were introduced for measuring the grasping force, suction strength, and contact on the tool part; therefore, the tool parts are not equipped with any electrical devices and, thus, can be easily sterilized. With these implementations, the surgeon can handle the master console wearing surgical gloves even during conventional surgery. For safe operation, pneumatic contact sensors were implemented between the operator's hands and the tool parts. In the case where the operator's hand is detached from the tool part, the manipulators are automatically locked by the brakes, and the software sends the locking status to the surgical robot.

Parallel mechanism

Requirements

First, we considered the design of the surgical robot to determine the master console design. According to the concept of a whole robotic system, only the tool manipulators on the surgical robot are controlled during the surgical procedure. The base robot is moved by foot switches; however, it is fixed during the procedure for safety. Therefore, the master manipulators are used only to control the tool manipulators on the surgical robot. Second, to design the master manipulator, we analyzed the motions involved in conventional brain tumor removal surgery. To realize the general input motions of conventional surgery, the manipulator requires 6-DOF full motion (translational and rotational) within a workspace of 50 mm × 50 mm × 50 mm for translations and ±90° for rotations. In addition, the workspaces of the two master manipulators are required to be placed close together to achieve conventional surgical motions. Furthermore, the master manipulator is required to be highly backdrivable since surgical tools can be moved freely in conventional surgery. Brakes to lock the master manipulator are also required for safety. Note that force feedback is not needed in this application; thus, the master manipulator is purely passive (not equipped with a motor). Therefore, we developed a new parallel mechanism taking into account these requirements.

Implementation

Parallel mechanisms generally enable lightweight and low-friction/inertia end effector by fixing the actuators and sensors to the base part. In this research, the master manipulator is purely passive; thus, none of the actuators are implemented. However, brakes and optical encoders should be implemented. As these components can be fixed to the base of the mechanism, the structure can be expected to be lightweight and robust. Therefore, the use of parallel mechanisms is a rational approach for fulfilling the requirements described above.

Our previously presented 3-DOF parallel mechanism, DELTA-R [12] (illustrated in the left panel of Fig. 4), has a significant advantage in its mechanical design as a two-arm configuration (in contrast, a conventional 3-DOF parallel mechanism such as DELTA has three arms). In the DELTA-R mechanism, a 15 % larger workspace, a 40 % smaller footprint, and most importantly, open access to the workspace in front of the device are obtained compared with the DELTA mechanism. In this research, we propose a new 5-DOF parallel mechanism that has the advantages of a two-arm configuration to avoid mechanical interference since the two

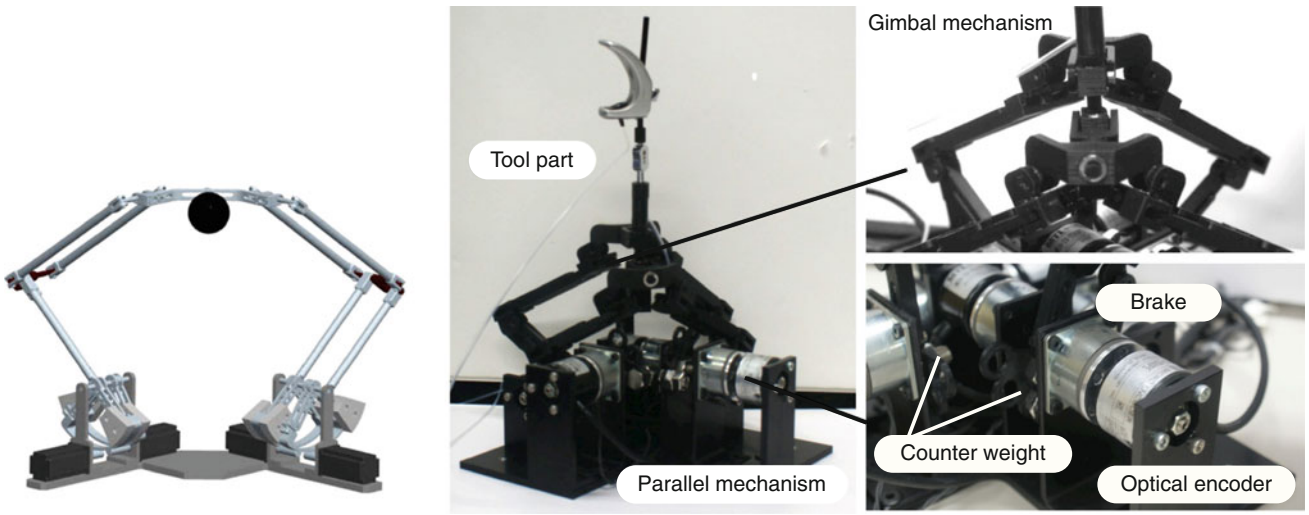

Fig. 4 The *left picture* shows our previously presented DELTA-R mechanism. The developed master manipulator consists of a parallel mechanism and a tool part. The *center* and *right pictures* show an overview of the manipulator and mechanical components

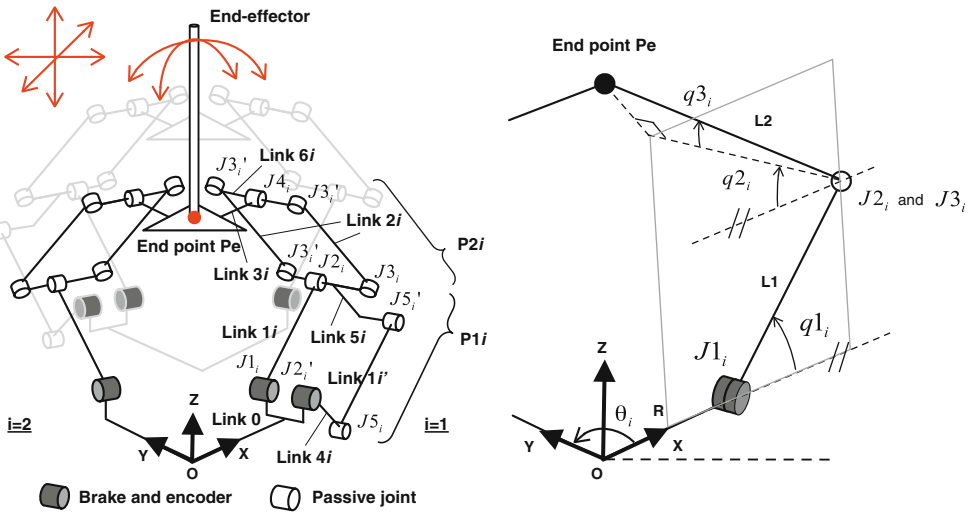

Fig. 5 The *left diagram* shows the kinematic model of the proposed parallel mechanism. The mechanism consists of a pair of modified DELTA-R mechanisms connected to each other by gimbal joints. The *right diagram* shows a simplified kinematic model of the modified DELTA-R. The forward kinematic model is given by solving a pair of modified DELTA-R mechanisms independently

manipulators should be placed close together to allow for conventional surgical motion. In the new parallel mechanism, a pair of 3-DOF modified DELTA-R mechanisms are both located in the same direction, and a pen-type end effector is attached through a gimbal joint from each end of the modified DELTA-R mechanism (illustrated in the center and right panels of Fig. 4). The 3-DOF translational motions can be given by the motions of the pair of modified DELTA-R mechanisms in the same direction, and the 2-DOF rotational motions can be given by the differential motions. Therefore, the end effector obtains a 5-DOF motion. The 3-DOF modified DELTA-R mechanism is an extension of DELTA-R and decreases the number of base joints from four to three since the redundancy is not required for this application. Note that the redundancy plays an important role mainly on the force producibility; however, since the master manipulator is purely passive, the force producibility is not the primary concern. A more detailed description of the force producibility of parallel mechanisms can be found in [13]. The most advantageous feature of this mechanism is that all of the mechanical links are located on one side, and therefore, the two master manipulators can be placed close together. In addition, since the control components (such as optical encoders and brakes) can be placed on the bottom and are not moved during the operation, the end effector can be lightweight and highly backdrivable. Also, the mechanism can robustly lock the position and posture of the end effector thanks to the six brakes attached to the base joints.

The forward kinematic model of the developed parallel mechanism is given by solving the two models of the modified DELTA-R mechanisms independently; then, we obtain the end effector's position and rotation from the endpoint ($\boldsymbol{P}_e$) of each mechanism. First, we determine the variables as follows: The lengths of Links 0, 1, 2, and 3 in the left panel of Fig. 5 are denoted as $L0$, $L1$, $L2$, and $L3$, respectively. The rotation angles about $J1_i$, $J2_i$, and $J3_i$ are denoted as $q1_i$, $q2_i$, and $q3_i$, respectively. The joint angles of $J2_i$ and $J2'_i$ are equivalent based on parallelogram $P1_i$. In these joints, angles $q1_1$, $q1_2$, and $q2_1$ can be measured by optical encoders attached to the base joints. Using these parameters, the kinematic model of the modified DELTA-R can be simplified and described as shown in the right panel of Fig. 5. In this simplified model, the length R in Fig. 5 can then be given as follows:

$$R = L0 - L3 \tag{1}$$

The position of joint $J2_i$ can be expressed as follows:

$$\boldsymbol{P}_{2i} = \begin{bmatrix} x_{2i} \\ y_{2i} \\ z_{2i} \end{bmatrix} = \begin{bmatrix} (R + L1C_{1i})C_{\theta_i} \\ (R + L1C_{1i})S_{\theta_i} \\ L1S_{1i} \end{bmatrix} \tag{2}$$

$\boldsymbol{P}_e$ exists on a crossing line between two spheres of diameter $L2$ centered on $J2_1$ and $J2_2$. Therefore, $\boldsymbol{P}_e$ can be obtained using the angle $q2_1$ of joint $J2_1$ by substituting in $\theta_1 = 0, \theta_2 = \pi/2$ from the prototype geometric conditions as follows:

$$\boldsymbol{P}_e = \begin{bmatrix} x_e \\ y_e \\ z_e \end{bmatrix} = \begin{bmatrix} \frac{D(-E_1+E_2+2y_{22}^2)+B_2(E_1-E_2)T_{21}-G}{F} \\ \frac{y_{22}^2(2D^2+C(E_1-E_2)-2B_2DT_{21})-DG+B_2T_{21}G}{Fy_{22}} \\ A - x_eT_{21} \end{bmatrix} \tag{3}$$

where

$$\begin{aligned}
j &= 1, 2, 3 \\
C_{ji} &= \cos(qj_i),\ S_{ji} = \sin(qj_i),\ T_{ji} = \tan(qj_i) \\
C_{\theta i} &= \cos(\theta_i),\ S_{\theta i} = \sin(\theta_i) \\
A &= z_{21} + x_{21}T_{21} \\
B_1 &= A - z_{21} \\
B_2 &= A - z_{22} \\
C &= 1 + T_{21}^2 \\
D &= x_{21} + B_1T_{21} \\
E_1 &= L2^2 - B_1^2 - x_{21}^2 \\
E_2 &= L2^2 - B_2^2 - y_{22}^2 \\
F &= 2(D^2 + Cy_{22}^2 + B_2T_{21}(-2D + B_2T_{21})) \\
G &= \sqrt{y_{22}^2(-C(E_1 - E_2)^2 + 4CE_1y_{22}^2 + 4D^2(E_2 + y_{22}^2) + 4B_2T_{21}(-D(E_1 + E_2) + B_2E_1T_{21}))}
\end{aligned}$$

From the forward kinematic model described earlier, we obtain the endpoints of the pair of modified DELTA-R mechanisms. Then, we obtain the end effector's position and rotation from the middle point and vector angle of these two endpoints, respectively.

A prototype of the mechanism was constructed of ABS (Acrylonitrile-Butadiene-Styrene) resin for weight savings. The size of the prototype is compact (170 mm in width, 190 mm in depth, and 150 mm in height) thanks to the new parallel mechanism. The workspace of the manipulator is 50 mm × 50 mm × 50 mm in translation and ±90° in pitch and yaw rotations (there is no limitation for the roll motion). An electromagnetic brake (112-03-12, Miki Pulley Co., Ltd., Japan) and an optical encoder (MEH-20-2500PE, MTL Co., Ltd., Japan) were implemented on each base joint. Therefore, the manipulator is capable of locking its position, and the accuracy of the position measurement is approximately 0.05 mm. The accuracy of 0.05 mm is not significantly high compared with conventional haptic devices. However, the accuracy can be easily improved by selecting higher resolution encoders according to requirements. The size and weight of these components are not tightly restricted for parallel mechanisms since they are fixed to the base. One of the modified DELTA-R mechanisms, shown in front in the left panel of Fig. 4, is approximately 40 % smaller than the one in back to avoid mechanical interference. The front and back modified DELTA-R mechanisms were positioned with left–right asymmetry to compensate for the mechanism asymmetry that can potentially deteriorate the backdrivability (illustrated with gray lines in the left panel of Fig. 5). Counterweights were introduced for gravity compensation on each modified DELTA-R mechanism. Therefore, the mechanisms can be moved freely without feeling the weight of the mechanism and tool parts. The counterweights are 27.3 and 54.6 g on the fronts and backs of the modified DELTA-R

mechanisms, respectively. The roll axis of the end effector can be measured by adding an optical encoder; however, since the surgical robot has only 5-DOF, the roll axis encoder was not implemented. Therefore, the prototype is capable of 6-DOF full motion, and the position is measurable in 5-DOF: three translational and two rotational (pitch and yaw). The minimum distance between the two master manipulators is 30 mm thanks to the new parallel mechanism. Note that the developed master manipulator is equipped with brakes; however, it is not equipped with motors for force feedback.

Tool part

Requirements

Based on the concept above, the tool part is the device that the surgeon directly handles during the surgical procedure while wearing surgical gloves. Therefore, the tool part must be compatible with sterilization. In addition, a user-friendly design based on the conventional neurosurgical tool is required.

Implementation

To realize a user-friendly interface, actual surgical tools (suction tube and bipolar forceps, Mizuho Co., Ltd., Japan) were attached to the tip of the tool part (Fig. 6). The tool part was fabricated using ABS resin.

Pneumatic sensors were implemented to measure the grasping force and suction strength. Air flow is provided by a vacuum pump and regulator at a pressure of 5 kPa. A flow meter enables the measurement of the air flow volume passing through the air tube embedded in the tool part. As a grasping force sensor, an embedded air tube on the tip of the bipolar forceps is pinched by the operator's motion; then, the air flow is varied according to the operator's pinching force. Conventional suction tools are generally equipped with a hole allowing the surgeon to manipulate the suction pressure by sliding his or her finger over the hole. The implemented suction sensor operates similarly by measuring the air flow volume using the same mechanical principle. In addition, a pneumatic contact sensor is implemented in the holders of each tool part. The contact sensor simply detects the surface contact between the air hole and the surgeon's hand. The contact sensor was capable of detecting the hand removal within 16.3 ms in our preliminary test (average of 10 trials). Therefore, the tool parts are not equipped with any electrical devices and, thus, can be easily sterilized. In addition, the vacuum pump in the controller can be replaced with a pump that is typically installed in an operating room.

Decoupling between the clean and non-clean parts is an essential strategy to be considered for the sterilization of medical devices. In this master manipulator, we decoupled these parts using a surgical nylon sheet (thickness of 300 μm) that covers the palm rest. The parallel mechanism and the tool part are fixed by Neodymium magnets over the sheet; therefore, these parts can be decoupled. In this manner, only the parallel mechanism is covered by a sterile cover, and the tool parts can be directly handled by the surgeon and provide an intuitive surgical interface. The adsorption force of the Neodymium magnets is sufficiently large for the fixation; thus, these two parts are tightly connected during their operation. According to our preliminary test, the adsorption force of the magnet was over 5 N, and we have not experienced an unexpected disconnection during any of the operations or evaluation tests described in this study.

Software

The control software was implemented on Windows XP, and the control routine was driven at 1 kHz. To establish a network connection between the master manipulator and the surgical robot, we introduced an open network protocol for medical devices (OpenIGTLink [14]) in the control unit. The data sending frequency is adjustable up to 1 kHz, and for the prototype implementation, the frequency was set to 100 Hz. The network interface was also implemented for connecting with other devices including the navigation software. As illustrated in the upper panel of Fig. 7, a network connection can be established to navigation software such as 3D slicer [15] and virtual endoscopy software such as NewVes [16] by introducing a virtual robot. A virtual robot is network software that converts the data format between the surgical robot format and the navigation software format. The virtual robot also allows multiple connections with other devices without an increase in CPU load on the control unit of the master console. The motion of the master manipulator can be seen on the navigation software in real time, and also, the software is compatible with the 3D patient model built from pre-operative MRI images for surgical simulation and training using NewVes [17].

Results

Operability evaluation

In a motion input device, backdrivability is essential for smooth motion. In addition, to realize a conventional surgical motion, the mechanical impedance of the device must be minimized. Therefore, we conducted a measurement of the resistance force to evaluate the backdrivability of the developed master manipulator.

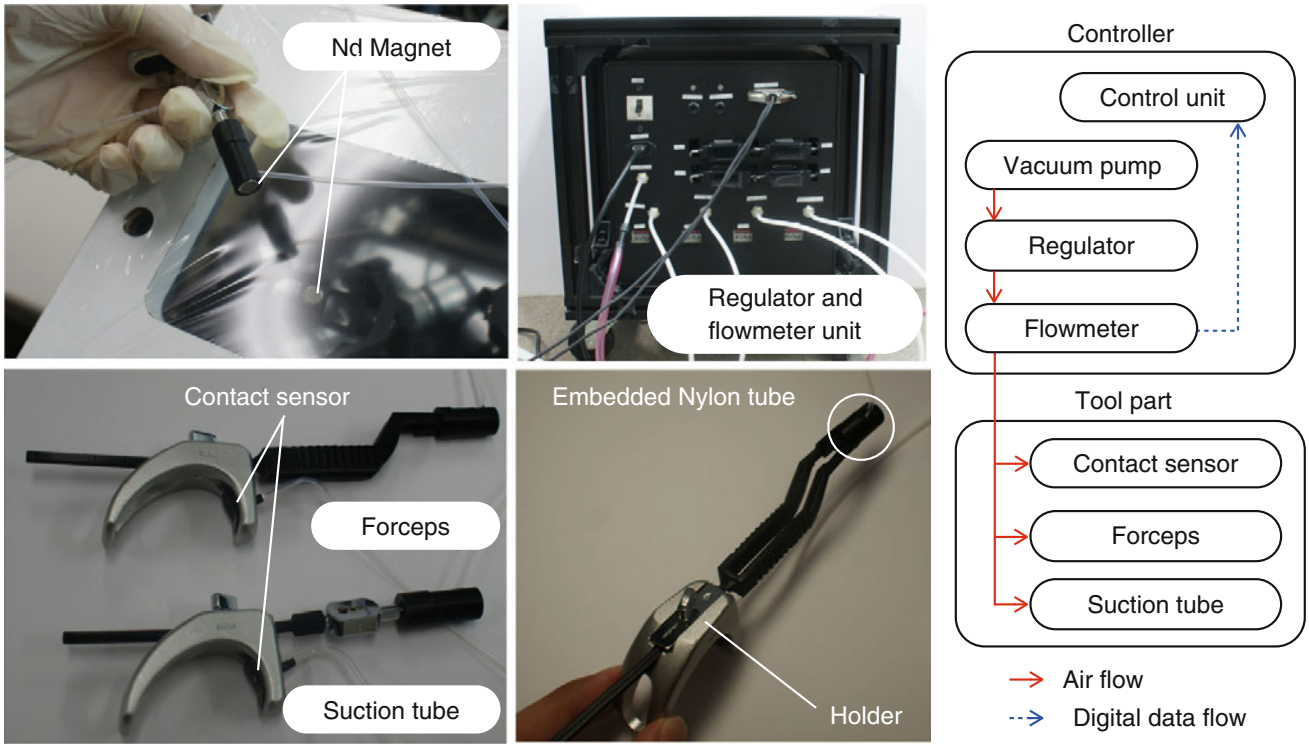

Fig. 6 The figures show the tool part setup. As shown in the *upper left picture*, the tool part is fixed to the manipulator using Neodymium magnets through a surgical drape. The grasping force, suction strength, and contact sensors were implemented using pneumatics. The *right schematic diagram* shows the system configuration of the pneumatic sensors

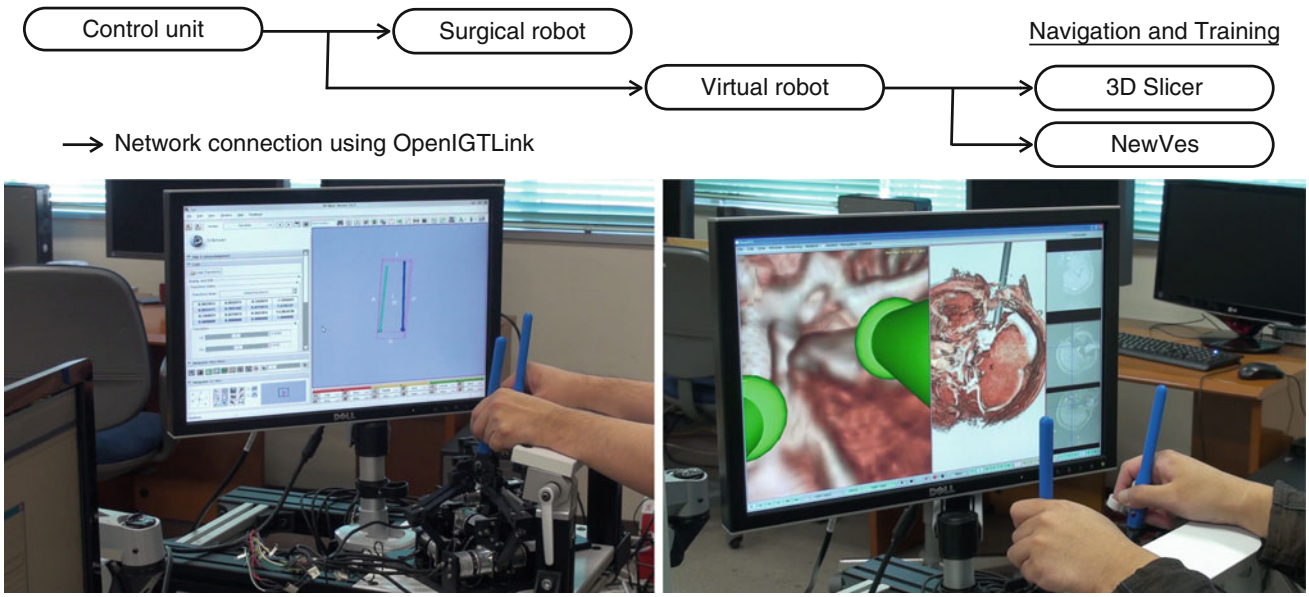

Fig. 7 The upper figure shows an overview of the network connection structure using OpenIGTLink. The *lower two pictures* show examples of collaboration with the 3D Slicer (*lower left*) and NewVes (*lower right*) navigation software packages. The tool parts in *blue* are the test tools without pneumatic sensors

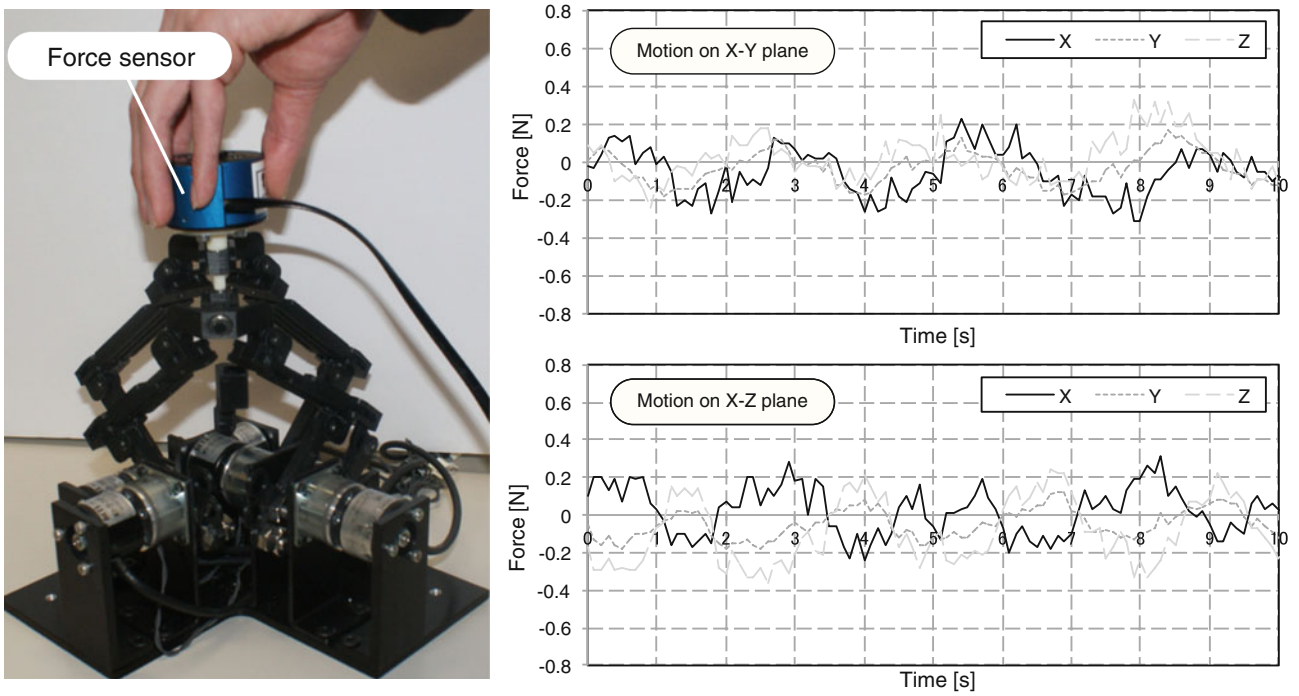

Fig. 8 The *left picture* shows the experimental setup. The *right graphs* show the experimental results for the resistance force observed during a simulated motion task. The results show the high backdrivability of the mechanism

Experimental setup

A 6-axis force sensor (IFS-50M31A25-I25, Nitta Corp., Japan) was attached to the end effector of the master manipulator and was grasped by the operator to measure the resistance force, as illustrated in the left panel of Fig. 8. A freehand circular motion (on the X–Y and X–Z planes) with a diameter of 15 mm and a period of 3 s was performed taking into account the actual surgical procedure. Note that these circular motions were approximate since they were performed by the operator.

Experimental result

The right panels of Fig. 8 show the experimental results. The resistance force was observed periodically in these results. When the peak value was observed at a point, the operator changed the direction. The main causes of the resistance force are assumed to be the inertia force and the static friction of the joints. The maximum resistance forces observed were 0.31, 0.16, and 0.33 N along the X, Y, and Z axes, respectively. The average of the maximum resistance forces along all axes was 0.27 N. From these results, it is revealed that the prototype realized a significantly high backdrivability. In addition, a sufficiently smooth motion input was confirmed by an experienced neurosurgeon in a qualitative assessment.

Pneumatic tool sensor evaluation

The usability of the tool part also strongly affects the operability of the master manipulator. Evaluation tests were conducted on the pneumatic sensors to show the operability of the tool parts mounted on the master manipulator.

Experimental setup

Evaluations of the grasping force and suction strength sensors were conducted. The grasping force sensor was tested using the experimental setup shown in the upper left panel of Fig. 9. The force was gradually applied to the forceps using a vice; then, the air flow volume was measured. The applied force was measured by a pressure sensor (LMA-A-20N, Kyowa Electronic Instruments Co., Ltd., Japan). For testing the suction strength sensor, the suction hole on the tool part was gradually covered, and the change in air flow volume was then measured. The experimental setup is shown in the lower left panel of Fig. 9. The measurements were conducted five times in both evaluation tests.

Experimental result

The experimental results for the grasping force sensor are shown in the upper right panel of Fig. 9. The measured air flow volume decreased when the applied load was over 3.5 N

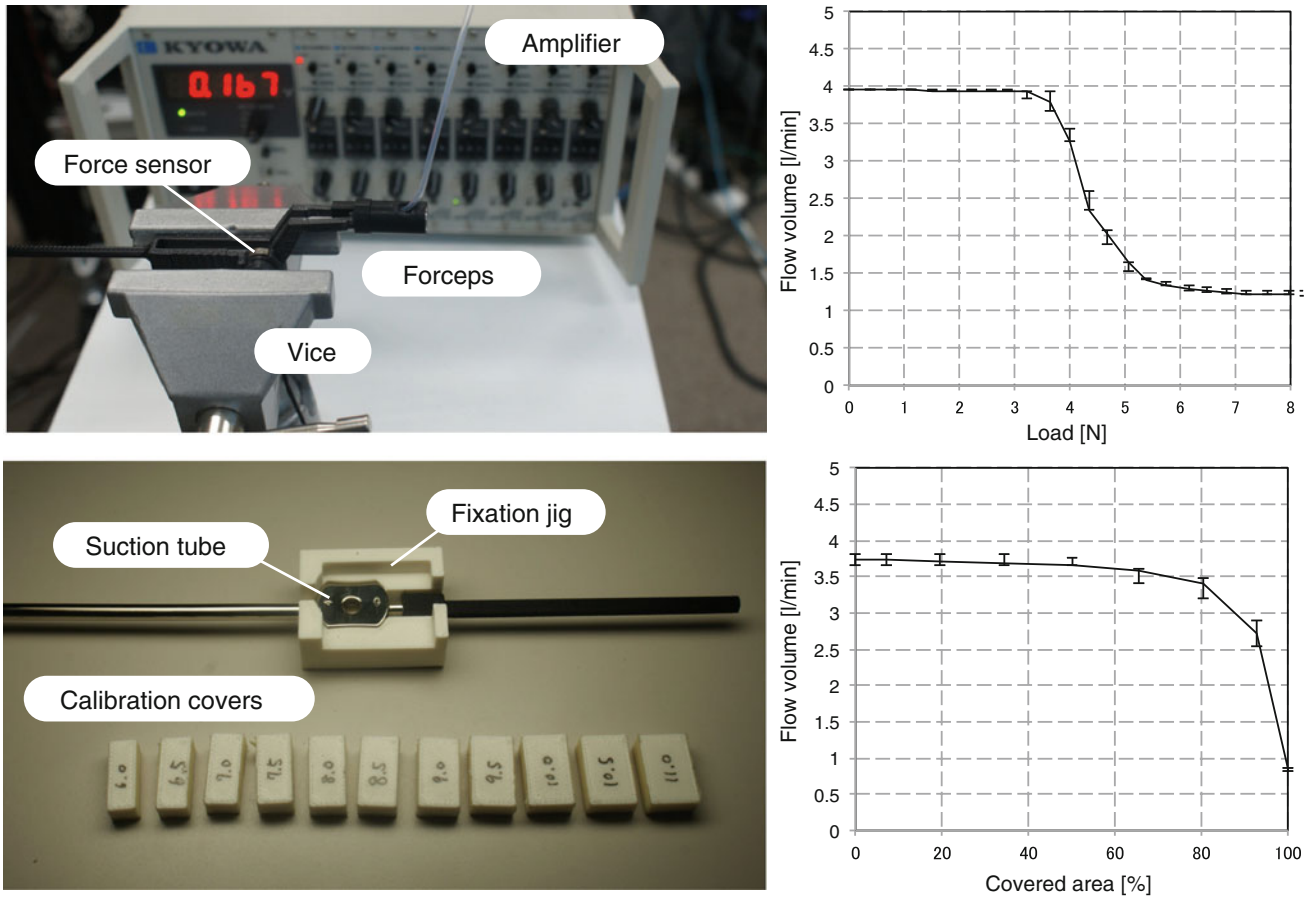

Fig. 9 The *upper picture* and *graph* show the experimental setup and the grasping sensor results, respectively. The *lower picture* and *graph* show the experimental setup and suction sensor results, respectively. Both experimental results show the effectiveness of the developed sensor

due to the elastic deformation of the forceps mechanism. Then, the air flow linearly decreased as the applied load increased to 5.5 N and stabilized at 1.25 l/min above 5.5 N. Therefore, the results show that the developed sensor can appropriately be used to detect the operator's grasping force.

The experimental results for the suction sensor are shown in the lower right panel of Fig. 9. From the experimental results, the air flow volume gradually decreased until 80 % of the covered area and then decreased at a steep angle over 80 up to 100 %. Since the sensor's mechanical principle is the same as for an actual suction tool, the characteristics shown in the results are supposed to already be incorporated in the human-in-loop system for experienced surgeons based on their experience. On the other hand, once the data are obtained by the sensor, a linearization of the sensor characteristics can be made by introducing a digital filter for further usability tuning.

Overall, the effectiveness of the pneumatic sensors was shown to be positive. In addition, the usability of the tool parts was highly regarded by an experienced neurosurgeon in a qualitative assessment.

Installability evaluation

To test the installability of the master console, the developed prototype was placed in an operating room, and a simulated conversion task between conventional and robotic surgery was performed. Figure 10 shows the surgical setup of the developed master console at the surgical bedside. In this test, the master console was fully covered with a surgical nylon drape as it would be in actual use. With the simulated conversion task, it was shown that the conversion required less than 60 s including the surgical robot setup. This result clearly shows that the system concept was properly implemented into the device's design.

The operability in an actual setting was also tested using the same experimental setup and showed the effectiveness of the device design to be positive. The input motion was intuitively performed based on the conventional surgical procedure, and the master console was sufficiently compact to be used in the surgical environment.

Fig. 10 The pictures show the experimental setup of the installability evaluation test. In this test, the master console was fully covered with a surgical nylon drape as it would be in actual use. The *left picture* shows the surgical setup for the robotic procedure. The *right two pictures* show motion input using the master console

Discussion

The technological contributions of this study are the newly developed compact 5-DOF parallel mechanism that realizes conventional neurosurgical motion and the pneumatic sensors that provide intuitive suction control and electric isolation for sterilization. These components were implemented in a desktop configuration; thus, the master console can be placed at the surgical bedside.

The 5-DOF parallel mechanism was developed for the master console to provide intuitive surgical motion inputs. The most advantageous feature of the mechanism is that the right and left arms can be placed close together (minimum distance of 30 mm) due to its compact and one-sided arm setup. In addition, the mechanism is capable of locking its position and rotation robustly thanks to the brakes fixed to the base joints. The evaluation tests of the master console clearly showed the effectiveness of our design. The resistance force of 0.27 N is significantly small even compared with cutting-edge haptic devices (e.g., the resistance force measured on Omega.3 that is a commercial haptic device (Force Dimension, Switzerland) [18] in the same experimental setup was 0.52 N in average). Note that a more detailed comparison between commercial haptic devices and DELTA-R, the predecessor of the proposed parallel mechanism, was described in [12]. However, a simple comparison cannot be made between the developed device and conventional haptic devices since the device is specialized for the surgical robotic system under development. Also the developed device is not exactly a haptic device since it is purely passive.

The developed pneumatic sensor plays a role in providing an intuitive interface and sterilizability. The mechanical principle of the pneumatic sensor is the measurement of air flow volume change caused by the user's input motion. The suction strength can be intuitively controlled as it is in the conventional surgical suction procedure by sliding a finger over the hole. The grasping force and contact with the tool can be measured using the same principle. The evaluation tests revealed that these sensors are capable of detecting user inputs. The time lag was 16.3 ms for the contact sensor in a preliminary test, and the brake activation time is 8 ms. Therefore, the device can be locked within 24.3 ms from the hand removal, which is sufficiently fast for the interface. In addition, since this principle does not require any electrical components, the tool part can be easily sterilized. The advantage of the proposed pneumatic sensor is also its compatibility

with the surgical environment since the vacuum pump is generally provided in the operating room.

The usability of the master console was highly regarded by an experienced neurosurgeon in a qualitative assessment. We consider that the developed parallel mechanism and pneumatic sensors largely contributed to the positive results. On the other hand, a further usability improvement is required on the master-slave control to realize a further intuitive operability. We are currently working on an evaluation of a master-slave system using the surgical robot. The kinematic model between the master-slave motion is one of our main interests to provide more intuitive operability into the system. Therefore, several series of tests are currently running to quantitatively assess the usability and to improve the robotic system.

Conclusion

In our research group, a robotic system for brain tumor removal is currently in development for complete brain tumor removal. The concept of the system is to combine conventional and robotic surgery to improve the tumor removal rate. The most advantageous feature of the proposed system is that the robot is compact and easily mounted on a conventional surgical head frame so that conversions between conventional and robotic surgery can be performed quickly. In this study, a newly developed master console for the robotic system designed based on the concept discussed earlier was described. The master console was developed taking into account the intuitive interface for surgeons based on conventional surgery and also the installability in the surgical environment. The evaluation tests and qualitative assessments from an experienced surgeon showed promising results.

Acknowledgments This study was funded by NEDO P10003 “Intelligent Surgical Instruments Project”, Japan.

Conflict of interest None.

References

1. The Committee of Brain Tumor Registry of Japan (2003) Report of Brain Tumor Registry of Japan (1969–1996). Neurol Med Chir Tokyo 43(suppl i–vii):1–111
2. Eljamel MS (2008) Robotic applications in neurosurgery. In: Medical robotics. InTech, Rijeka, pp 41–64
3. Zamorano L, Li Q, Jain S, Kaur G (2004) Robotics in neurosurgery: state of the art and future technological challenges. Int J Med Robot Comput Assist Surg 1(1):7–22
4. Cossu M, Cardinale F, Castana L, Citterio A, Francione S, Tassi L, Benabid AL, Russo LG (2005) Stereoelectroencephalography in the presurgical evaluation of focal epilepsy: a retrospective anal s of 215 procedures. Neurosurgery 57(4):706–718
5. Eljamel MS (2007) Validation of the PathFinder™ neurosurgical robot using a phantom. Int J Med Robot Comput Assist Surg 3(4):372–377
6. Guthart GS, Salisbury JK (2000) The intuitive telesurgery system: overview and application. In: Proceedings of international conference on robotics automation 2000, pp 618–621
7. Sutherland GR, Latour I, Greer AD (2008) Integrating an image-guided robot with intraoperative MRI: a review of the design and construction of neuroArm. IEEE Eng Med Biol Mag 27:59–65
8. SensAble Technologies. http://www.sensable.com/. Accessed 2 March 2012
9. Morita A, Shigeo S, Mitsuishi M (2005) Microsurgical robotic system for the deep surgical field: Development of a prototype and feasibility studies in animal and cadaveric models. J Neurosurg 103(2):320–327
10. Goto T, Hongo K, Kakizawa Y (2003) Clinical application of robotic telemanipulation system in neurosurgery. J Neurosurg 99(6):1082–1084
11. Arata J, Tada Y, Kozuka H, Wada T, Saito Y, Ikedo N, Hayashi Y, Fujii M, Kajita Y, Mizuno M, Wakabayashi T, Yoshida J, Fujimoto H (2011) Neurosurgical robotic system for brain tumor removal. Int J CARS 6(3):375–385
12. Arata J, Kondo H, Ikedo N, Fujimoto H (2011) Haptic device using a newly developed redundant parallel mechanism. IEEE Trans Robot 27(2):201–214
13. Arata J, Ikedo N, Fujimoto H (2011) Force producibility improvement of redundant parallel mechanism for haptic applications. In: Proceedings of international conference on intelligent robots and systems 2011, pp 2145–2150
14. Tokuda J, Fischer GS, Papademetris X, Yaniv Z, Ibanez L, Cheng P, Liu H, Blevins J, Arata J, Golby AJ, Kapur T, Pieper S, Burdette EC, Fichtinger G, Tempany CM, Hata N (2009) OpenIGTLink: an open network protocol for image-guided therapy environment. Int J Med Robot Comput Assist Surg 5(4):423–434
15. 3D Slicer. http://www.slicer.org/. Accessed 2 March 2012
16. Hayashi Y, Mori K, Fujii M, Kajita Y, Ito E, Takebayashi S, Mizuno M, Wakabayashi T, Yoshida J, Suenaga Y (2009) Virtual surgiscope: 3D visualization tool for assisting image-guided neurosurgery. Int J CARS 4(sppl 1):S246–S247
17. Hayashi Y, Takagi M, Arata J, Tokuda J, Yamada A, Hata N, Chinzei K, Kajita Y, Fujii M, Mizuno M, Wakabayashi T, Yoshida J, Mori K (2011) Development of endoscopic robot surgery simulation system using OpenIGTLink. J JSCAS 13(3):226–227 (in Japanese)
18. Force dimension. http://www.forcedimension.com/. Accessed 2 March 2012